energies

MDPI

Article

Optimal Scheduling of Multi-Energy Complementary Systems Based on an Improved Pelican Algorithm

Hongbo Zou [1,3], Jiehao Chen [1], Fushuan Wen [2,*], Yuhong Luo [1], Jinlong Yang [1] and Changhua Yang [1]

[1] College of Electrical Engineering and New Energy, China Three Gorges University, Yichang 443002, China; zhbhorace@ctgu.edu.cn (H.Z.); yruuchan@163.com (J.C.); luoyuhong_203@163.com (Y.L.); yangjl25@163.com (J.Y.); 18385615363@163.com (C.Y.)
[2] Hainan Institute, Zhejiang University, Sanya 572025, China
[3] Hubei Provincial Key Laboratory for Operation and Control of Cascaded Hydropower Station, China Three Gorges University, Yichang 443002, China
* Correspondence: fushuan.wen@gmail.com

Abstract: In recent years, the global power industry has experienced rapid development, with significant advancements in the source, network, load sectors, and energy storage technologies. The secure, reliable, and economical operation of power systems is a critical challenge. Due to the stochastic nature of intermittent renewable energy generation and the coupled time-series characteristics of energy storage systems, it is essential to simulate uncertain variables accurately and develop optimization algorithms that can effectively tackle multi-objective problems in economic dispatch models for microgrids. This paper proposes a pelican algorithm enhanced by multi-strategy improvements for optimal generation scheduling. We establish eight scenarios with and without pumped storage across four typical seasons—spring, summer, autumn, and winter—and conduct simulation analyses on a real-world case. The objective is to minimize the total system cost. The improved pelican optimization algorithm (IPOA) is compared with other leading algorithms, demonstrating the validity of our model and the superiority of IPOA in reducing costs and managing complex constraints in optimization.

Keywords: renewable energy; economic dispatch; multi-objective optimization; power system cost reduction

check for updates

Academic Editor: Adolfo Dannier

Received: 3 December 2024
Revised: 4 January 2025
Accepted: 13 January 2025
Published: 16 January 2025

Citation: Zou, H.; Chen, J.; Wen, F.; Luo, Y.; Yang, J.; Yang, C. Optimal Scheduling of Multi-Energy Complementary Systems Based on an Improved Pelican Algorithm. *Energies* **2025**, *18*, 365. https://doi.org/10.3390/en18020365

Copyright: © 2025 by the authors. Licensee MDPI, Basel, Switzerland. This article is an open access article distributed under the terms and conditions of the Creative Commons Attribution (CC BY) license (https://creativecommons.org/licenses/by/4.0/).

1. Introduction

In response to global climate change, China is committed to achieving its "dual-carbon" goals, driving the need for innovative energy solutions. With the increasing demand for energy and a growing emphasis on renewable sources, multi-energy complementary systems have emerged as a promising approach for efficient energy supply. This system integrates various forms of energy, including wind, solar, hydroelectric, thermal power generation, and energy storage, to optimize scheduling and achieve efficient energy utilization while ensuring stable system operation.

The multi-energy complementary system facilitates the synergistic use of diverse energy sources, enabling flexible scheduling based on actual demand and resource availability. This integration not only enhances energy efficiency but also reduces operational costs, lessens reliance on traditional energy sources, and mitigates environmental pollution. Among these energy sources, pumped storage stands out as a low-carbon, flexible regulation option with mature technology and significant development potential. By harnessing its energy storage capabilities, pumped storage can smooth the fluctuations of wind and

photovoltaic generation, thereby minimizing disruptions to the safe and stable operation of the power supply system.

Despite the advancements in scheduling optimization methods for multi-energy complementary systems, significant research gaps remain. Existing optimization techniques often suffer from limitations in efficiency and flexibility, failing to adequately address the complexities of modern energy demands. Consequently, there is a pressing need for improved scheduling algorithms that can effectively coordinate the diverse energy sources within these systems.

This study introduces the intelligent multi-energy complementary optimization algorithm (IPOA), a novel scheduling algorithm designed to enhance the efficiency of energy utilization within multi-energy systems. The IPOA integrates multiple energy sources, such as wind, solar, hydro, and thermal energy, to optimize energy allocation and reduce operational costs. By promoting low-carbon development and providing effective solutions for climate change challenges, this research contributes to the advancement of multi-energy complementary systems and supports the transition to sustainable energy practices.

2. Literature Review

The stability and economics of power systems are largely affected by the inherent stochasticity, intermittency, and volatility of wind and PV power output. To address this issue, capacity planning models for energy storage systems are crucial. In [1], a planning model focusing on a coordinated scheduling strategy considering generation and operating reserves in a wind–PV–pumped storage system is presented, which aims to minimize the renewable energy curtailment and the total operating cost of each generation unit. Similarly, in [2], a capacity allocation optimization model for a hybrid hydropower–PV–storage system was proposed, which emphasizes economic optimization under multiple constraints. Furthermore, in [3], an artificial sheep algorithm utilizing improved artificial sheep algorithms was used to study the optimal allocation of installed capacity of various power sources in a clean energy complementary base. The impacts of various parameters on the allocation of installed capacity and the importance of considering factors such as power supply guarantee and power abandonment rates are demonstrated in these studies. In [4], a related study focusing on the optimal economic allocation strategy of a hybrid energy storage system for mitigating wind power fluctuations is presented, where by analyzing the frequency-domain characteristics of wind power, the authors determine the optimal cut-off frequency and operating period for the energy storage system. In the field of energy management systems, several studies have focused on similar optimization problems. In [5], an improved particle swarm optimization (IPSO) algorithm is used to propose an optimal allocation model for energy storage in distribution networks. By considering both economic and stability factors, the capacity allocation problem of each unit is successfully optimized so that voltage stability is enhanced and the cost of energy storage is reduced. In [6], an improved NSGA-II method is proposed, which takes the highest wind power regulation rate, the lowest output fluctuation, and the lowest operation cost of pumped storage as the optimization objectives to pre-dispatch the bundled wind power generation system. The experimental results show that pumped storage has great benefits for the economy of the multi-energy system.

In [7], the water cycle algorithm (WCA), which is an optimization method with many iterations and slow convergence speed, is proposed to optimize the scheduling of the microgrid and reduce operating cost and environmental pollution to the maximum extent. The results show that the scheduling results of this algorithm are more economical than other mainstream algorithms. In [8], an improved immune particle swarm algorithm is proposed, which is documented with optimal economics and minimum output power

fluctuation of the combined wind storage system as the objective function, and the results show that the whole combined system will be optimized with the addition of pumped storage. In [9], an enhancement for artificial neural network (ANN) using particle swarm optimization (PSO) is proposed to manage renewable energy resources (RESs) in a virtual power plant (VPP) system, and the load demand test is carried out for 24 h and the optimal energy scheduling of the microgrid is realized through hourly weather data. In [10], a multi-objective evolutionary algorithm based on Pareto optimal space with NDWA-GA and PCA is proposed and the objective function is set to minimize the economic cost and the battery capacity, the proposed wind power–photovoltaic storage model in this study has the lowest economic cost with accurate prediction of hydropower plant output. In [11], an adaptive fractional-order algorithmic strategy and a multi-objective classification algorithm are used to solve a multi-objective optimization problem with the objective function set to maximize the combined generation capacity and minimize the system power fluctuation, which provides a reference for the future implementation of a joint dispatch strategy for a hydropower plant, neighboring wind farms, and photovoltaic farms. In [12], a two-delay deep deterministic policy gradient algorithm (TD3) was used to compare three scenarios under different energy storage operations, and by comparing different scenarios, a reliable, economical, and environmentally friendly hybrid energy storage system was constructed.

In recent years, convex relaxation techniques have emerged as a powerful tool for addressing the non-convexity of optimization problems in microgrid economic dispatch. For instance, in [13], Liang et al. proposed a steady-state convex bi-directional converter model, enabling high-efficiency economic dispatch in hybrid AC/DC networked microgrids. This approach effectively transforms non-convex problems into convex formulations, significantly enhancing computational efficiency while ensuring global optimality. In summary, these papers highlight the importance of developing optimization models for energy storage systems in the context of renewable energy integration, emphasizing the need to consider factors such as economic efficiency, system stability, and fluctuation mitigation, which collectively contribute to the optimization of the energy storage capacity of a wind–solar interconnected system, and demonstrating the importance of effective capacity allocation to improve the overall performance and economic viability of the system. By analyzing the fluctuations of wind and solar energy and utilizing the regulation capability of pumped storage, the optimal installed capacity allocation scheme is solved and obtained. The importance of developing optimization models for energy storage systems in the context of renewable energy integration is jointly emphasized in these papers, where factors such as economic efficiency, system stability, and degree of fluctuation should be focused on, and these literature studies demonstrate the importance of effective capacity allocation in wind–solar hybrid systems to improve the overall system performance and economic viability.

In addition, studies on multi-objective optimization algorithms to optimize the scheduling of multi-energy systems containing wind, solar, hydro, thermal and storage resources are also current research topics, and some of the studies provide valuable insights into similar areas. In [14], a competitive mechanism-integrated multi-objective equilibrium optimization algorithm was used to propose an optimal scheduling strategy for smart buildings with photovoltaic energy storage systems. In [15], a multi-objective optimal scheduling strategy for a renewable energy distribution network was developed, and the operational efficiency of a multi-energy system was improved after being solved by this improved genetic algorithm. Furthermore, in [16], a multi-objective particle swarm optimization-based algorithm was used to solve the optimal scheduling of a wind–solar–storage system. In [17], an optimal scheduling strategy emphasizing a global optimization model and a Pareto optimal solution screening method for wind–solar–solar and multi-

type energy storage co-generation systems was proposed. In [18], a day-ahead scheduling and real-time dispatch model was developed to optimize the use of renewable energy sources while minimizing the operating costs, focusing on the coupling between cooling and power energy sources within a microgrid. In [19], a novel MOWSO algorithm has been proposed, and the results indicate that a well-organized energy storage charge and discharge can effectively mitigate power fluctuation in the microgrid, particularly when there is significant fluctuation in load and new energy power with low matching degree, considering the operating cost, carbon emission, and power fluctuation of the microgrid as the objective function. Together, these studies have contributed to the development of optimal scheduling methods for wind–water–fire multi-energy complementary systems. By addressing various optimization challenges and emphasizing the efficient use of renewable energy sources, researchers are paving the way for sustainable and cost-effective integration of multiple energy resources. These studies highlight the importance of multi-objective optimization algorithms in improving the operational efficiency, economic viability, and environmental sustainability of complex energy systems. By employing advanced algorithms and strategic optimization methods, researchers are paving the way for more efficient use of renewable energy sources and energy storage technologies for the optimization of novel power systems.

Although significant progress has been made in optimizing multi-energy systems, several research gaps remain. First, many existing optimization algorithms, such as particle swarm optimization and genetic algorithms, struggle with convergence speed and solution accuracy when addressing complex, multi-objective problems involving renewable energy integration. Second, while convex relaxation and similar approaches have been effective in simplifying optimization problems, their application is often limited to specific scenarios and lacks generalizability to systems with dynamic and nonlinear constraints. Lastly, few studies have explored the integration of advanced metaheuristic algorithms, such as the improved pelican optimization algorithm (IPOA), in addressing real-world challenges in multi-energy complementary systems. This study addresses these gaps by proposing the IPOA as a robust optimization framework tailored to improve the scheduling and performance of such systems under realistic operational constraints. This study focuses on optimizing the design and medium-term planning of microgrid systems incorporating renewable energy sources. The methodology is applicable to systems where long-term operational patterns are of interest rather than real-time intraday scheduling tasks. While a detailed intraday scheduling model would involve mixed-integer programming to account for unit states, startup costs, and spinning reserves, this study simplifies the problem to evaluate the performance of the IPOA under dynamic constraints and multi-objective scenarios.

The lack of binary variables to represent unit states is a deliberate simplification, justified by the study's focus on planning-scale decisions rather than detailed operational scheduling. Future work will extend this methodology to mixed-integer programming formulations, enabling its application to more granular intraday scheduling problems.

3. Theoretical Analysis

To study the output power characteristics of renewable energy sources such as wind, solar, and water, most of the existing studies have focused on a system of wind, solar, and water alone, or a complementary power generation system between two energy sources such as wind, solar, and water, while there are fewer studies on wind and water multi-source complementary power generation systems. The active power output characteristics of wind, solar, water, and other energy sources have different complementary characteristics at different time scales. It is the research direction of this chapter to analyze the comple-

mentary characteristics of wind, solar, and water at different time scales. Recently, many research studies have included a focus on wind, solar, and water multi-source complementary co-generation systems, showing that multi-energy complementary power generation systems fully leverage the natural complementary advantages of energy, improve energy utilization efficiency and power supply reliability, and can greatly reduce environmental pollution and the curtailment rate of wind and solar energy.

3.1. Multi-Energy Complementary Power Generation System

A multi-energy complementary system is a power system that includes wind power, photovoltaic power, hydropower, and other energy sources based on the complementary characteristics of multiple energy sources in different time and space scales, combining the resource conditions and local energy characteristics of each place, adapting to local conditions, optimizing the combination of multiple energy sources such as wind energy, solar energy, hydropower, and fossil fuels, supplementing it with an energy storage system, planning for the construction of various types of power sources in a holistic manner, and rationally scheduling various types of power sources in order to promote the capacity of renewable energy consumption and realize the best overall economic efficiency and green sustainable development, so the multi-energy complementary system is superior in terms of environmental protection, economy, safety and reliability, independence and flexible scheduling. The details are shown in Figure 1.

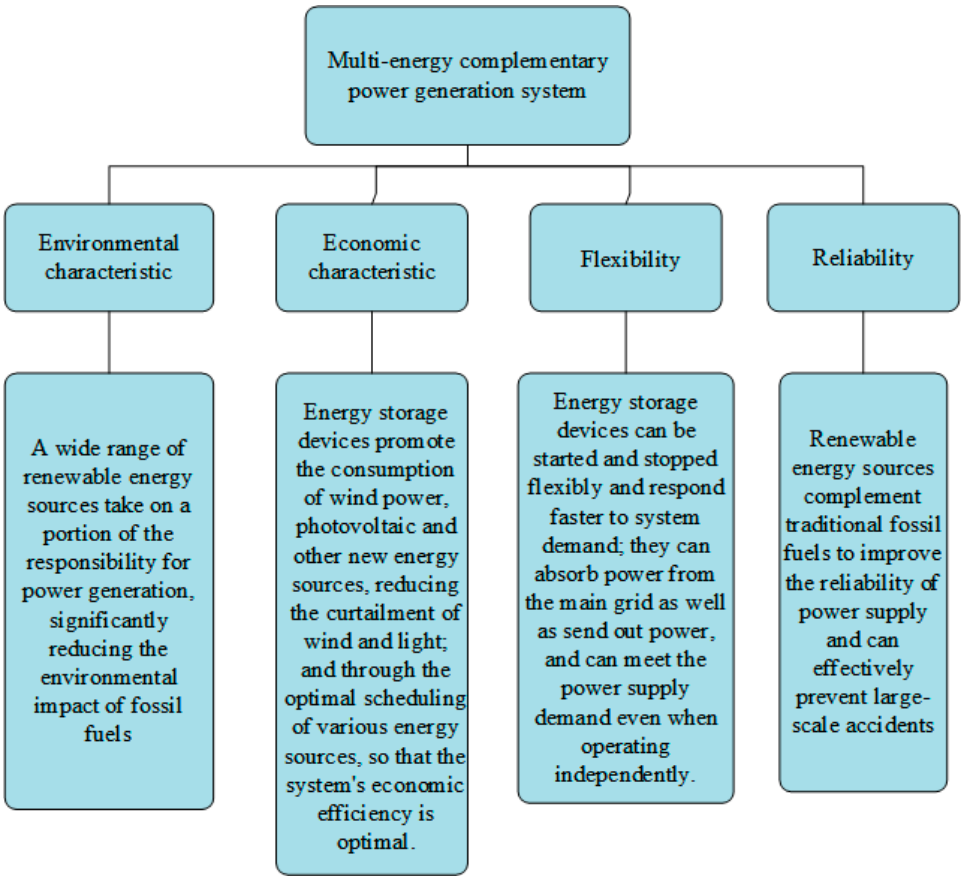


Figure 1. Characteristics of the microgrid.

3.2. Wind–Solar–Water Output Characteristics

3.2.1. Wind Power Output Characteristics

The power output of wind farms is mainly affected by changes in air density and wind speed, which are natural factors that are usually unchangeable by human beings, so the

accuracy of wind power output prediction has a very important impact on the optimal scheduling of multi-energy complementary systems. The wind speed follows a Weibull distribution with typical daily and seasonal characteristics, and the output power of a wind farm is usually determined by the wind speed. The expressions for wind speed and wind farm output power are detailed in reference [10].

The historical data of wind power generation in four seasons of a year are selected to analyze its output characteristics, and the wind power output is shown in Figure 2.

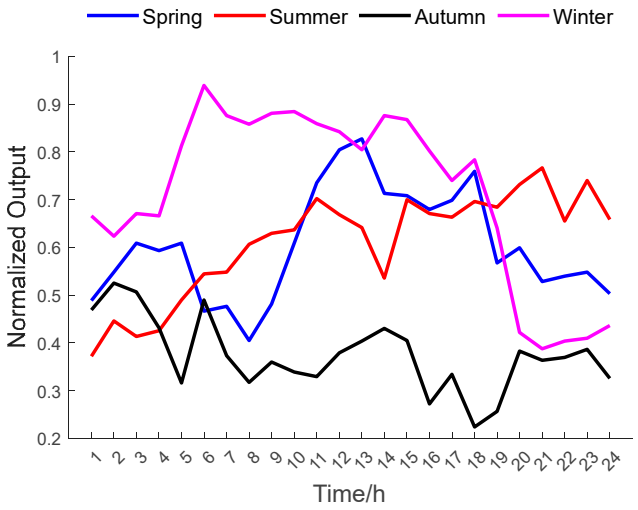


Figure 2. Wind power output variation curve during a certain day in spring, summer, autumn, and winter.

The large rate of change of wind power output is not only manifested in its daily output characteristics, but also in its seasonal output characteristics. Wind power seasonal characteristics are significant, so different seasons should be considered separately. Wind power generated by natural wind has a very large impact on power volatility, specifically reflected in the large daily rate of change and seasonal rate of change, showing a strong seasonal intermittency. Due to the different seasons, its daily power rate of change is also very large. Figure 2 provides a wind power curve analysis for a region during the four seasons of spring, summer, fall and winter on a certain day. The vertical axis represents the normalized output (dimensionless), calculated by dividing the instantaneous power output by the maximum possible output of the respective energy source.

3.2.2. Photovoltaic Output Characteristics

The output power of photovoltaic power stations is affected by the local solar radiation intensity and environmental temperature; the specific formula for calculating output power can be found in reference [20]. The output characteristics of photovoltaic power are traceable and obvious and should be considered separately in conjunction with different time periods when load peaks occur. As shown in Figure 3, the daily output waveform of photovoltaic units on four typical days of spring, summer, autumn, and winter is measured at a point every hour. The specific situation is demonstrated below.

From Figure 3, it can be seen that the PV output has the characteristics of daytime generation and nighttime shutdown, and the overall change takes the shape of a bell, but due to the PV output by the weather and cloud cover, with randomness and volatility, the specific output has jagged fluctuations. In different seasons, due to different solar intensities, the generation of PV power in the afternoon peak period is not the same.

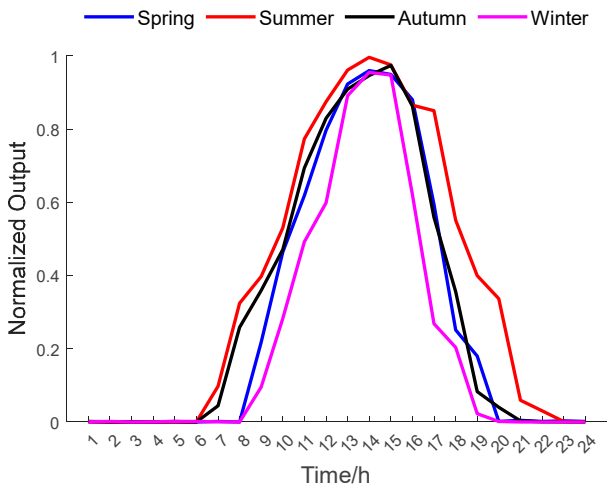


Figure 3. Photovoltaic output variation curve during a certain day in spring, summer, autumn, and winter.

3.2.3. Hydroelectric Output Characteristics

The power generation of hydroelectric units is mainly determined by their net head, efficiency, and water consumption. The head does not change much within a day, so the net head and efficiency in this article are generally constant. The actual output power of the hydroelectric units is shown in reference [21]. Due to the differences in geographic location and rainfall time, the power output of hydropower is different in different seasons of the year, and four typical days of spring, summer, fall, and winter are selected to analyze the characteristics of its hydropower output, as shown in Figure 4.

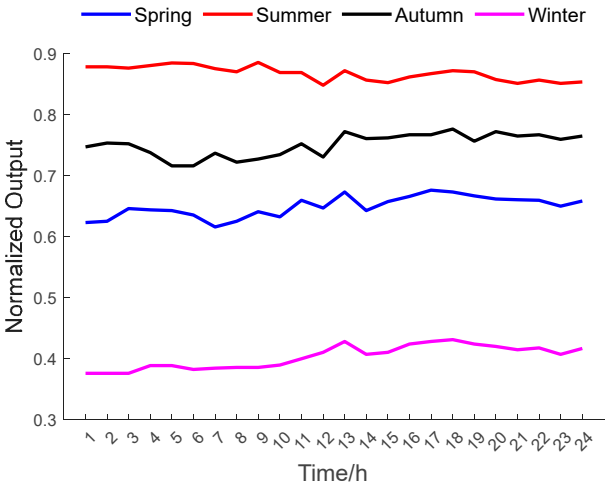


Figure 4. The output variation curve of hydropower during a certain day in spring, summer, autumn, and winter.

Hydropower output during the year is significant, with hydropower being abundant during the flood season and water being scarcer during the non-flood season for hydropower. Therefore, the hydropower output is larger during the flood season and generally carries the base load, while the hydropower output is smaller during the non-flood season. As can be seen from the above figure, the region is non-flooded in winter and flooded in spring and summer. For hydropower units in the non-flood season, peak capacity takes on the peak load or waist load; in the flood season, in order to reduce water abandonment, it mainly takes on the base load. This often leads to

insufficient peaking capacity during the flood season and insufficient peaking power during the non-flood season.

3.3. Wind–Solar–Water–Storage Complementarity

Using the wind and hydropower output model to simulate the corresponding annual output process of wind power, photovoltaic power, and hydropower, and analyzing the complementary characteristics at different scales between wind and hydropower, it can be found that wind power and photovoltaic output have natural spatio-temporal complementarities. In references [22–25], multi energy complementary systems are widely used as models for solving and verifying this statement. In terms of time, from the monthly time-scale perspective, wind energy is stronger in winter, the temperature is lower, the solar time is shorter, and the solar energy is weaker, while wind energy is weaker in summer, the temperature is higher, the daytime is longer, and the solar energy is stronger, so the wind and solar energy have better complementary characteristics in summer and winter. From the daily time-scale perspective, sunny days have abundant solar energy and weaker wind energy, while cloudy and rainy days are exactly the opposite, with weaker solar energy and stronger wind energy. From the hourly time-scale perspective, the output of photovoltaic power plants is concentrated during the day, and the output of wind turbines is relatively small, while at night, the output of photovoltaic power plants is zero, and the output of wind turbines is relatively large. From a spatial-scale perspective, wind and solar energy distributed over a wide area in the northern mainland and the eastern coast of China have good spatial complementarity at all time scales, and the larger the area over which the two renewable energy sources are dispersed, the stronger the spatial complementarity at the daily and hourly time scales. Wind power and hydropower also show good complementary properties in time. Often winter and spring wind energy is abundant and water resources are in short supply, while summer and fall are rich in water resources and poor in wind energy; thus, building a wind–water complementary system that can improve the peak-regulating capacity of hydropower while making full use of wind power resources is important.

In terms of regulation capacity, a good complementarity is also found among wind power, photovoltaic power, and hydropower. The output of wind and photovoltaic power is mainly related to the environmental temperature, solar radiation, and weather changes, so it shows obvious daily and seasonal cycle characteristics and has a strong intermittency and volatility, as well as poor controllability. The strong controllability and good regulation ability of hydropower are acknowledged, and the regulating capacity of hydropower can be freely adjusted within a certain range and is not completely affected by natural precipitation and river runoff. Compared with the independent hydropower station, the gradient of the small hydropower group is more closely related to both electricity and hydropower, and through the reasonable and optimized scheduling of hydropower stations at all levels, the water resources of the whole basin can be effectively utilized. From the perspective of instantaneous regulation, it is recognized that the hydropower unit possesses good climbing ability, short response time, fast regulation rate, and a wide adjustable range, and has good complementarity with wind and photovoltaic power, which have strong intermittency and volatility. The fluctuation of wind and solar output is suppressed, and the output curve of the power generation alliance is smoothed.

4. Materials and Methods

The selection of the improved pelican optimization algorithm (IPOA) as the core method in this study is based on its unique advantages in addressing complex, multi-objective optimization problems. Compared to traditional optimization methods such

as particle swarm optimization (PSO) and genetic algorithms (GAs), the IPOA exhibits superior convergence speed and solution accuracy due to its multi-strategy enhancements, including nonlinear weighting factors, Cauchy variation, and the sparrow alert mechanism. These features enable the IPOA to avoid local optima and achieve better performance under the dynamic and nonlinear constraints typical of multi-energy complementary systems.

Other alternatives, such as convex relaxation techniques, are effective in transforming non-convex problems into solvable convex forms. However, their applicability is often limited to specific problem types, whereas IPOA offers a more generalizable and adaptive framework for solving highly constrained, real-world problems.

By incorporating the IPOA, this study contributes to the literature by demonstrating its applicability in realistic scenarios, providing a robust optimization framework that effectively balances computational efficiency and solution precision. These characteristics position the IPOA as a significant advancement over traditional methods in optimizing multi-energy complementary systems. Although the POA, like other metaheuristic algorithms, is designed to avoid local optima, its standard version may still suffer from premature convergence under complex, high-dimensional optimization problems with nonlinear constraints. This limitation arises from its relatively simple exploration and exploitation mechanisms, which may lack the adaptability required for highly constrained multi-objective problems. To address this, the improved pelican optimization algorithm introduces enhancements such as nonlinear weighting, Cauchy variation, and a sparrow alert mechanism. These modifications significantly improve the algorithm's ability to escape local optima and achieve global optimal solutions in dynamic and nonlinear optimization scenarios.

4.1. Objective Function

With the rapid development of renewable energy, widespread attention has been given to wind and solar energy as the two predominant forms of renewable energy. However, due to their fluctuating and intermittent characteristics, the instability of wind and solar energy represents a significant challenge to their large-scale application. To overcome this problem, researchers have begun to explore multi-energy complementary power generation systems that combine wind and photovoltaic energy with other forms of energy, such as hydropower, thermal energy, and energy storage, aiming to enhance the reliability, stability, and economic viability of the system.

In the domestic context, the Chinese government places great emphasis on the development of renewable energy and has implemented a series of policy measures to promote the construction of multi-energy complementary power generation systems. For example, the National Energy Administration (NEA) has issued the Renewable Energy Power Development Plan (2016–2030), which outlines the goal of actively developing wind, solar, and hydro energies, and encourages the use of multi-energy complementary power generation systems to achieve efficient utilization and optimal energy allocation.

The total system cost is a critical consideration in the design of a multi-energy complementary power generation system. Since the construction, operation, and maintenance costs of different energy forms vary, it is a key issue to determine how to minimize the total cost while ensuring system performance. Researchers seek an optimal balance between economic viability and technical feasibility by employing multi-objective optimization algorithms, such as the improved NSGA-II (improved non-dominated sorting genetic algorithm). By considering factors such as investment and operational and maintenance costs of different energy forms, the optimal scheduling and configuration of a multi-energy complementary power generation system can be achieved, thereby reducing the total cost of the system.

Another critical consideration is the impact of wind and solar power output volatility on system returns. Given the volatility of wind and solar energy, the power generation capacity of the system fluctuates across different time periods. Therefore, it is essential to strategically utilize other forms of energy to mitigate the adverse effects of wind and solar volatility on system returns. A common approach involves integrating hydro and thermal energy as auxiliary sources to ensure a stable power supply. Furthermore, the application of energy storage technologies can effectively smooth wind–solar volatility and enhance system reliability. By optimizing scheduling algorithms and energy management strategies, researchers can maximize the complementarities among wind, solar, hydro, thermal, and storage energies to maximize the system benefits.

In summary, given the domestic context, the criticality of total system cost, and the potential gains from wind and solar volatility, the research on multi-energy complementary power generation systems has garnered widespread attention in China. Therefore, this issue focuses on two main objective functions: minimizing the total system cost and minimizing the volatility of wind and solar energy.

4.1.1. Total Cost

The objective function requires that the total cost of the system is minimized and the equation is shown below:

$$\min C = \sum (C_w + C_{pv} + C_h + C_{pump}) - \sum (I_{ELE} + I_{cap} + I_w + I_{pv} + I_h) + C_{pun} + C_{rs} - C_{eb} \quad (1)$$

where C_w, C_{pv}, C_h, and C_{pump} are the cost of operation in wind power plants, photovoltaic power plants, hydroelectric power plants, and pumped storage power plants, respectively; I_{ELE} and I_{cap} are, respectively, the power and capacity revenues from the two-part tariff; I_w, I_{pv}, and I_h are, respectively, the proceeds from the sale of wind power, photovoltaic power, and hydroelectric power; C_{pun} is the penalty for curtailment of wind and solar energy; C_{rs} is the cost of the system spinning reserve; and C_{eb} is the environmental benefits.

Among them,

$$I_{ELE} = \sum_{t=1}^{T} (C_{pump} \cdot P_{pump}^t \cdot \mu_p - C_{turbine} \cdot \frac{P_{turbine}^t}{\mu_t}) \quad (2)$$

where μ_p and μ_t are, respectively, the generation efficiency and pumping efficiency of the pumped storage power plant; C_{pump} and $C_{turbine}$ are, respectively, the selling price and the purchasing price of electricity at time t; and P_{pump}^t and $P_{turbine}^t$ are, respectively, the pumping power as well as the generation power at moment t.

$$I_{CAP} = C_{cap} \cdot P_{pump_max} \quad (3)$$

where C_{cap} is the price per unit capacity of the pumped storage power plant, and P_{pump_max} is the maximum capacity of the pumped storage power plant.

$$I_w = \sum_{t=1}^{T} c_w \times P_w^t \quad (4)$$

$$I_{pv} = \sum_{t=1}^{T} c_{pv} \times P_{pv}^t \quad (5)$$

$$I_h = \sum_{t=1}^{T} c_h \times P_h^t \quad (6)$$

where c_w, c_{pv}, and c_h are, respectively, the selling prices of wind power, photovoltaic power, and hydroelectric power at moment t; and P_w^t, P_{pv}^t, and P_h^t are, respectively, the power generation of wind power, photovoltaic power, and hydroelectric power at moment t.

$$C_{pun} = \rho_{w,pv} \times (\sum_{t=1}^{T} P_{curt}^{wind}(t) - \sum_{t=1}^{T} P_{curt}^{pv}(t)) \quad (7)$$

where $\rho_{w,pv}$ is the cost coefficient of wind and solar energy curtailment, taking a value of 1.2 CNY/kWh; and $P_{curt}^{wind}(t)$ and $P_{curt}^{pv}(t)$ are, respectively, the amount of wind and solar energy curtailment at moment t.

$$C_{rs} = \sum_{t=1}^{T} \rho_{res} \times (e_D P_{D,t} + e_w P_{w,t} + e_{pv} P_{pv,t}) \quad (8)$$

where ρ_{res} is the rotating standby cost factor; and e_D, e_w, and e_{pv} are, respectively, the forecast error rates for load, wind, and photovoltaic power.

$$C_{eb} = \sum_{t=1}^{T} (\rho_w P_{w,t} + \rho_{pv} P_{pv,t} + \rho_{pump} P_{pump,t} + \rho_h P_{h,t}) \quad (9)$$

where ρ_w, ρ_{pv}, ρ_{pump}, and ρ_h are, respectively, the coefficients of wind power, photovoltaic, pumped storage, and load impact on environmental benefits.

The hydroelectric conversion relationship is given by

$$P_{h,j,t} = \xi_{1j}(U_h^t)^2 + \xi_{2j}(Q_{j,t})^2 + \xi_{3j} U_h^t Q_{j,t} + \xi_{4j} U_h^t + \xi_{5j} Q_{j,t} + \xi_{6j} \quad (10)$$

4.1.2. Scenic Volatility

The standard deviation is one of the statistical quantities that describes the distribution of data or the degree of concentration of a sample. It measures the difference or dispersion between a data value and its mean. The larger the standard deviation, the more dispersed the data point is from the mean; the smaller the standard deviation, the less dispersed the data point is from the mean. In this paper, the standard deviation of wind–solar–water output is used as an evaluation index of wind–scenery volatility. The formula is shown below:

$$\min V = \sqrt{\frac{\sum_{t=1}^{T} (P_{W,t} + P_{H,t} + P_{S,t} - P_{L,t} - P_{av})}{T}} \quad (11)$$

$$P_{av} = \frac{\sum_{t=1}^{T} (P_{W,t} + P_{H,t} + P_{S,t} - P_{L,t} - P_{av})}{T} \quad (12)$$

where $P_{W,t}$, $P_{H,t}$, and $P_{S,t}$ are the generation power of wind power, pumped storage, and photovoltaic at time t, respectively; $P_{L,t}$ is the load power at time t; and P_{av} is the average value of the power in time T.

4.2. Constraints

1. Power balance constraint:

$$P_{L,t} = P_{w,t} + P_{pv,t} + P_{h,t} + P_{turbine,t} - P_{pump,t} \quad (13)$$

where $P_{L,t}$, $P_{w,t}$, $P_{pv,t}$, $P_{turbine,t}$, and $P_{pump,t}$ represent load, wind power, photovoltaic power, hydropower, pumped storage power, and pumped storage pumping, respectively.

2. Pumped storage constraints:

$$u^t_{pump} + u^t_{turbine} \leq 1 \tag{14}$$

$$0 \leq P^t_{turbine} \leq u^t_{turbine} \times P^{max}_{turbine} \tag{15}$$

$$0 \leq P^t_{pump} \leq u^t_{pump} \times P^{max}_{pump} \tag{16}$$

$$Q_{phs(0)} = Q_{phs(24)} = 0.35 Q_{phsN} \tag{17}$$

where u^t_{pump} means pumping and $u^t_{turbine}$ means generating (both can only be '0' or '1'); $P^t_{turbine}$ and P^t_{pump} represent the actual power generation and pumping power of pumped storage, respectively; and $Q_{phs(t)}$ represents the amount of water stored at moment t.

3. Wind, solar, and water output constraints:

$$\begin{cases} 0 \leq P^t_w \leq P^{max}_w \\ 0 \leq P^t_{pv} \leq P^{max}_{pv} \\ 0 \leq P^t_h \leq P^{max}_h \end{cases} \tag{18}$$

where P^t_w, P^t_{pv}, and P^t_h denote wind power, photovoltaic power, and hydroelectric power, respectively.

4. Climbing rate constraints for thermal power units:

$$\begin{cases} P_{gi,t} - P_{gi,t-1} \leq r_{gi,up} \\ P_{gi,t-1} - P_{gi,t} \leq r_{gi,down} \end{cases} \tag{19}$$

where $P_{gi,t}$ and $P_{gi,t-1}$ denote the output of thermal unit i at moment t and moment t-1, respectively, and $r_{gi,up}$ and $r_{gi,down}$ denote the upper and lower creep rate limits, respectively.

5. System positive and negative spinning backup constraints:

$$\begin{cases} \sum_{i=1}^{N_G} (P_{gi,max} - P_{gi,t}) \geq \mu_{d1} P_{D,t} + \mu_{w1} P_{W,t} + \mu_{pv1} P_{PV,t} \\ \sum_{i=1}^{N_G} (P_{gi,t} - P_{gi,min}) \geq \mu_{d2} P_{D,t} + \mu_{w2} P_{W,t} + \mu_{pv2} P_{PV,t} \end{cases} \tag{20}$$

where $P_{gi,max}$ and $P_{gi,min}$ denote the upper and lower output limits of thermal unit i, respectively; μ_{d1}, μ_{w1}, and μ_{pv1} are positive rotating reserve capacity factors to cope with load, wind, and PV forecast errors; and μ_{d2}, μ_{w2}, and μ_{pv2} are negative rotating reserve capacity factors to cope with load, wind, and PV forecast errors.

6. Transmission capacity constraints:

$$0 \leq P_{w,t} + P_{pv,t} + P_{h,t} + P_{turbine,t} \leq P_{L,max} \tag{21}$$

7. Hydroelectric generation constraints:

$$U^{min}_{j,t} \leq U^t_{j,t} \leq U^{max}_{j,t} \tag{22}$$

$$U^t_{j,t} = U^{t-1}_{j,t} + I_{j,t} + (Q_{j-1,t} - Q_{j,t}) \tag{23}$$

$$Q_{min} \leq Q_{j,t} \leq Q_{max} \tag{24}$$

where $U^t_{j,t}$ and $Q_{j,t}$ are the reservoir capacity and outflow from the hydropower plant at moment t, respectively, and $I_{j,t}$ is the amount of water coming from the hydropower plant at moment t.

5. Pelican Optimization Algorithm Based on Multi-Strategy Improvement

5.1. Pelican Optimization Algorithm (POA)

The pelican optimization algorithm (POA) is a heuristic intelligent optimization algorithm proposed in 2022, which is inspired by the smart and natural hunting behaviors of pelicans while catching fish. The algorithm consists of three phases: the population initialization phase, the exploration phase, which imitates the behavior of pelicans moving towards prey, and the development phase, which imitates the behavior of pelicans skimming the water surface. The POA is a population-based algorithm, which is mainly characterized by fast convergence speed, high accuracy of searching for optimal results, fewer setup parameters, and a wide range of applications compared to other different algorithms. In this subsection, the stages of the pelican optimization algorithm are described in detail.

5.1.1. Stock Initialization Phase

Assuming that there are n pelicans in the m-dimensional space and the position of the i-th pelican in the m-dimensional space is $X_i = [X_{i1}, X_{i2}, \cdots, X_{in}]$, the mathematical modeling of the position X_i of all the pelicans can be expressed as a matrix with n rows and m columns:

$$X = \begin{bmatrix} (X_1) \\ (X_2) \\ \vdots \\ (X_n) \end{bmatrix} = \begin{bmatrix} X_{11} & \cdots & X_{1m} \\ \vdots & \ddots & \vdots \\ X_{n1} & \cdots & X_{nm} \end{bmatrix} \tag{25}$$

The initialization formula is

$$x_{ij} = l_j + \alpha \cdot (U_j - l_j), i = 1, 2, \cdots, n; j = 1, 2, \cdots, m \tag{26}$$

where x_{ij} is the position of the i-th pelican in the j-th dimension; n is the population size of the pelicans; m is the dimension of the solution problem; α is a random number in [0, 1]; and U_j and l_j are the upper and lower bounds of the solution problem in the j-th dimension, respectively.

5.1.2. Exploration Phase

In the first phase, the pelican determines the location of its prey and then moves towards the identified area. By modeling this strategy of the pelican, the search space can be scanned, thus improving the search capability of the POA in terms of discovering different regions of the search space. In each iteration, the mathematical model of the new position of the pelican is represented in the following equation:

$$x_{ij}^{p1} = \begin{cases} x_{ij} + \sigma \cdot (P_j - I \cdot x_{ij}), F_p < F_j \\ x_{ij} + \sigma \cdot (x_{ij} - P_j), F_p \geq F_j \end{cases} \tag{27}$$

where x_{ij}^{p1} is the position of the i-th pelican in the j-th dimension after the first-stage update, σ is a random number in the range of [0, 1], I is a random integer in the range of [1, 2], P_j is the position of the prey in the j-th dimension, and F_p is the value of the objective function of the prey.

If the value of objective function F_p is improved at position i, the position is updated with the following equation:

$$x_i = \begin{cases} x_i^{p1}, F_i^{p1} < F_i \\ x_i, F_i^{p1} \geq F_i \end{cases} \tag{28}$$

where x_i^{p1} is the new position of the i-th pelican; x_i is the new position of the i-th pelican after the first-stage update; and F_i^{p1} is the objective function of the i-th pelican at the new position after the first-stage update.

5.1.3. Development Phase

In the second stage, the pelican reaches the surface of the water, spreads its wings above the surface to grab the fish out upwards, and then takes the prey into its throat pouch. This attack strategy leads to more fish being caught in the attack area, and simulating this behavior allows the POA to converge to better points within the hunting area, which enhances the algorithm's local ability of searching and utilization. In each iteration, the mathematical model of the new position of the pelican is represented in the following equation:

$$x_{ij}^{p2} = x_{ij} + R \cdot (1 - \frac{t}{T}) \cdot (2 \cdot \beta - 1) \cdot x_{ij} \tag{29}$$

where x_{ij}^{p2} is the position of the i-th pelican in the j-th dimension after the second-stage update, β is a random number in [0, 1], R is a random integer of 1 or 2, t is the number of current iterations, and T is the maximum number of iterations.

If the value of objective function F_p is improved at position i, the position is updated with the following equation:

$$x_i = \begin{cases} x_i^{p2}, F_i^{p2} < F_i \\ x_i, F_i^{p2} \geq F_i \end{cases} \tag{30}$$

where x_i^{p2} is the new position of the i-th pelican; x_i is the new position of the i-th pelican after the second-stage update; and F_i^{p2} is the objective function of the i-th pelican at the new position after the second-stage update.

5.2. Pelican Algorithm Based on Multi-Strategy Improvement

Although the traditional POA is a metaheuristic algorithm, it suffers from low solution accuracy, lack of stability, and slow convergence speed, and it can easily fall into the local optimal solution, making it difficult to meet the demands of solving complex power system optimization and scheduling problems with multiple objectives, nonlinearity, and multiple constraints. In order to improve the speed and accuracy of the algorithm, this paper optimizes the POA by introducing the nonlinear weight factor, Cauchy variation strategy, and sparrow alert mechanism, which improve the algorithm's solution accuracy and prevent the algorithm from falling into the local optimal solution. This paper also adopts Skew Tent mapping for population initialization to improve the global convergence speed of the algorithm. Based on the above series of optimization of the algorithm, this paper proposes an improved pelican algorithm (IPOA) based on fusion of the sparrow vigilance mechanism and Cauchy variation optimization. In this section, the principle of the IPOA and the main improvement strategies are described in detail.

5.2.1. Tent Mapping-Based Population Initialization

Chaotic systems are characterized by randomness, regularity, and ergodicity, and the chaotic sequences generated by chaotic systems can better initialize the distribution of the initial population individuals. Currently, the commonly used chaotic mapping methods are logistic mapping, Tent mapping, and circle mapping.

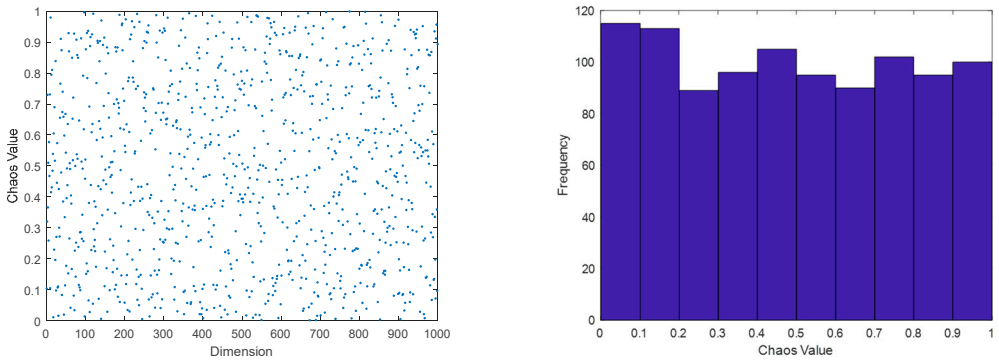
Since the initial population of the POA is randomly generated, the uniform distribution of the initial positions of individuals in the search space cannot be guaranteed, which has adverse influences on the search speed and optimization performance of the algorithm.

Therefore, Tent mapping is introduced in the initialization process of IPOA to increase the traversability of the initial population.

$$x_i = l_b + (u_b - l_b) \cdot z_i \tag{31}$$

$$z_{i+1} = \begin{cases} \frac{z_i}{\alpha} & , x_i \in [0, \alpha) \\ \frac{1-z_i}{1-\alpha} & , x_i \in [\alpha, 1) \end{cases} \tag{32}$$

where x_i is the position of the i-th pelican; l_b is the lower limit of the variable boundary; u_b is the upper limit of the variable boundary; z_i is the chaotic sequence; and α is a constant, which is generally taken as 0.3. The Tent mapping diagram is shown in Figure 5.



(**a**) (**b**)

Figure 5. Tent mapping diagram. (**a**) Reflection on the Relationship between Particle Dimensions and Chaos Values, (**b**) Reflection on the Relationship between Chaos Value and Frequency.

5.2.2. Introducing a Nonlinear Weighting Factor in the Exploration Phase

The local optimization ability and global search ability of the coordination element heuristic algorithm are the key factors affecting the optimization accuracy and speed of the algorithm. Since the update of individual pelican position is closely related to the current pelican position, a nonlinear inertia weighting factor is used to adjust the correlation between the update of pelican position and the information on current pelican position.

At the beginning of the algorithm iteration, the value of ω is low, and the update of the optimal individual position is less affected by the current pelican position, which is allows the algorithm to search in a wider range and improves the algorithm's global development ability. As the optimization process progresses, the value of ω becomes higher, the update of the optimal individual position is more affected by the current pelican position, and the optimization range of the algorithm reduces, which helps the algorithm to search for the optimal solution. Through this improvement, not only has the local exploration ability of the algorithm been improved, but also the local exploration ability of the algorithm has been enhanced. The formula is as follows:

$$\omega = \frac{e^{\frac{t}{T}} - 1}{e - 1} \tag{33}$$

where t is the current number of iterations and T is the maximum number of iterations.

5.2.3. Introducing the Cauchy Variation Strategy in the Development Phase

In the development phase of the pelican algorithm, the Cauchy variation strategy is introduced. The size of the current fitness value is compared with the average fitness value of the population in each iteration. When the pelican fitness value is higher than the average fitness value of the population, it means that the current locations of pelicans are concentrated, and at this time, the Cauchy variation strategy is introduced to increase the

diversity of pelicans. When the pelican fitness value is lower than the population average fitness value, the original pelican location update method is used.

The Cauchy variation distribution function is as follows:

$$p = \frac{1}{2} + \frac{1}{\pi}\arctan\frac{\gamma}{g} \tag{34}$$

$$\gamma = \tan(\pi \times (p - 0.5)) \tag{35}$$

whose corresponding density function is

$$\text{Cauchy}(\gamma) = \frac{1}{\pi} \times \frac{g}{g^2 + \gamma^2} \tag{36}$$

The position update formula is

$$X_{new} = X_{best} + \text{Cauchy}(\gamma) \cdot X_{best} \tag{37}$$

where g is a scale parameter, which has a value greater than 0, and p is a random number uniformly distributed between [0, 1].

5.2.4. Sparrow Alert Mechanism

The sparrow alert mechanism is introduced to the development phase of the POA. Incorporating the pelican into the sparrow's alert mechanism makes the convergence speed of the POA faster. Pelicans at the edge of the flock will move quickly to the safe area to achieve a better position when they realize the danger, and pelicans located in the middle of the flock will walk randomly to get closer to other pelicans.

The position update formula is shown below:

$$x_{i,j}^{t+1} = \begin{cases} x_{best,j}^{t} + \beta \times \left| x_{i,j}^{t} - x_{best,j}^{t} \right|, f_i < f_g \\ x_{i,j}^{t} + K \times \left(\frac{\left| x_{i,j}^{t} - x\omega_j^{t} \right|}{(f_i - f_\omega) + \varepsilon} \right), f_i = f_g \end{cases} \tag{38}$$

where $x_{best,j}^{t}$ is denoted as the j-th dimension of the global optimal position when the number of iterations is t; β is a step adjustment parameter obeying a normal distribution with mean 0 and variance 1; K is a random number in the range of $[-1, 1]$; ε is a non-zero constant set to a size of 10^{-50}; f_i is the fitness value of the current individual; f_g is the value of global optimal individual fitness of the current iteration; and f_w is the value of global worst individual fitness of the current iteration.

5.3. Calculation Process

The specific calculation steps of the IPOA are as follows:

1. Set the relevant parameters such as population size N, iteration number T, upper and lower limits of variables, dimensionality, and so on.
2. Initialize the population using Tent chaotic mapping.
3. Calculate the fitness value of the population.
4. Generate prey randomly.
5. Introduce the nonlinear weight factor and enter the first stage: calculate the position of the i-th pelican in the j-th dimension according to Equation (27).
6. According to the formula, determine whether the position needs to be updated or not, and end the first stage.
7. Enter the second stage: introduce the Cauchy variation strategy and the sparrow alert mechanism, and calculate the position of the i-th pelican in the j-th dimension.

8. According to the formula, judge whether the position needs to be updated and end the second stage.
9. Judge whether the end condition is satisfied; input the next step if it is satisfied, and return to Step 4 if it is not satisfied.
10. Output the optimal solution.

According to the above steps, the flowchart of the algorithm can be drawn as Figure 6.

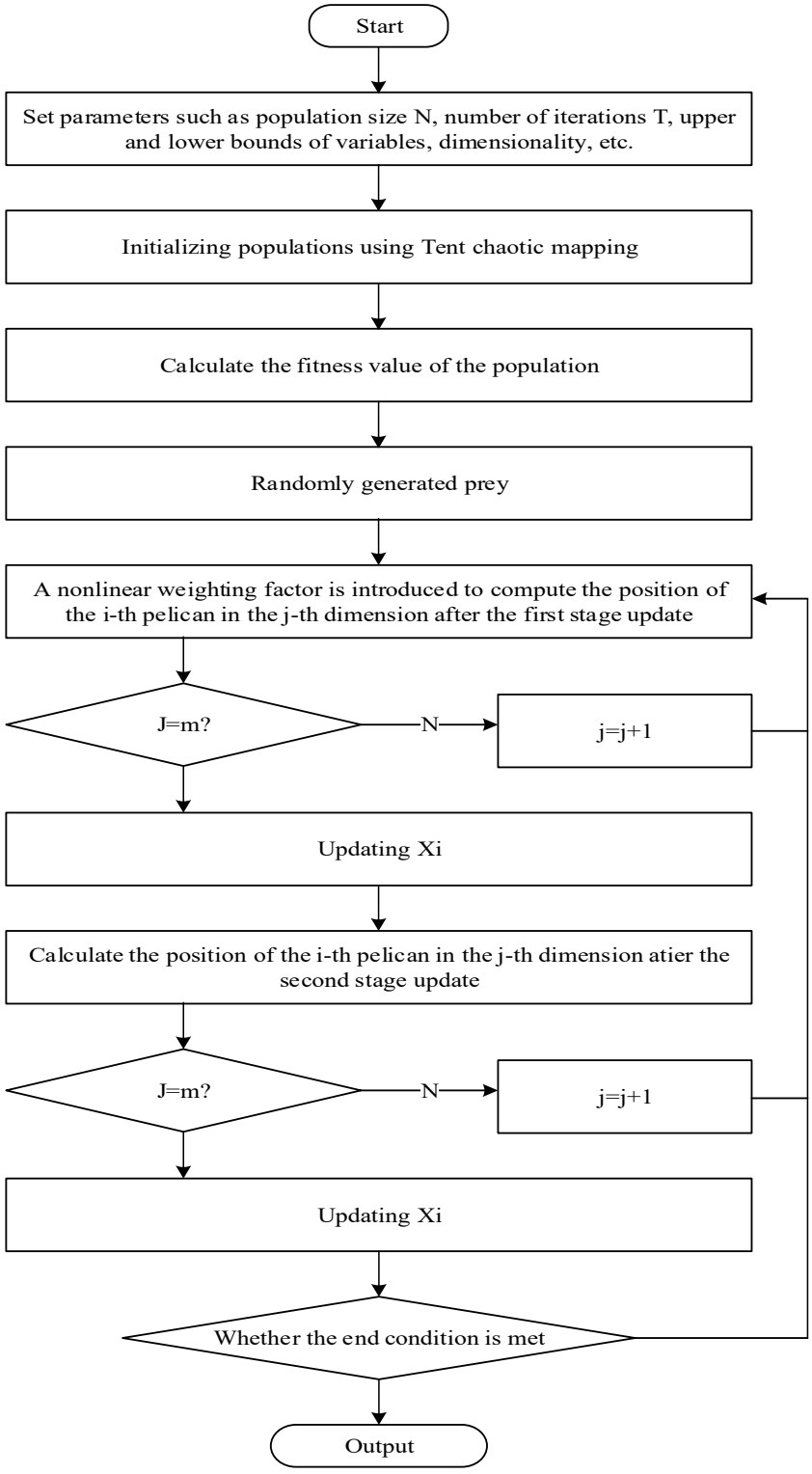


Figure 6. Calculation flowchart of the IPOA.

5.4. Algorithm Testing and Analysis

In CEC2022, F3, F6, F10, and F11 are selected as functions, the number of populations is set to 30, the dimension is set to 20, and the maximum number of iterations is set to 1000, and each algorithm is run 30 times, respectively. The results of several algorithms are compared and analyzed.The results are shown in Figure 7:

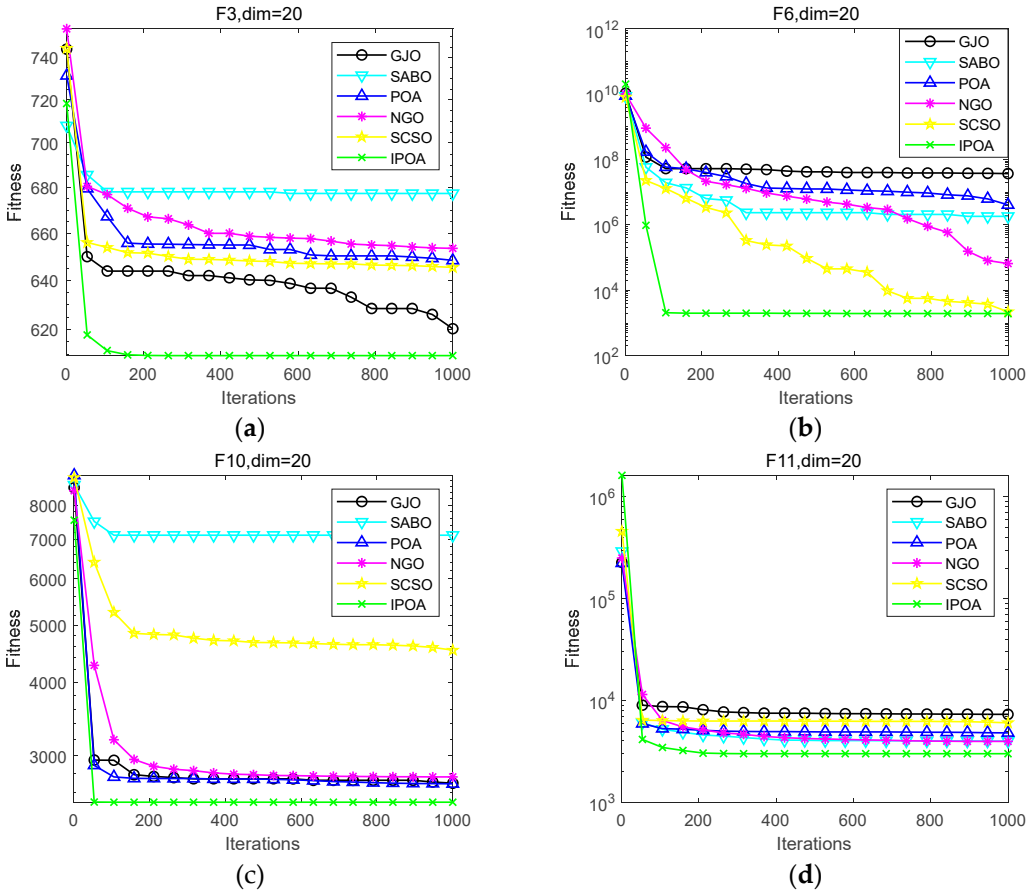


Figure 7. Comparison of algorithm results. (**a**) Comparison of convergence speed of 6 algorithms in function F3, (**b**) Comparison of convergence speed of 6 algorithms in function F6, (**c**) Comparison of convergence speed of 6 algorithms in function F10, (**d**) Comparison of convergence speed of 6 algorithms in function F11.

To compare the calculational effectiveness of the IPOA and other algorithms, experimental section time is needed. The average time for calculating F3, F6, F10, and F11 using IPOA, PSO, WOA, and POA is 8.93 s, 10.82 s, 15.3 s, and 9.02 s, respectively. These findings highlight IPOA's ability to balance solution quality and computational speed, making it suitable for large-scale and time-sensitive applications.

The following figure shows the standard deviation of each algorithm in the test functions F1-F12, the degree of dispersion of the objective value after the algorithm optimizes the function is reflected by the value of the standard deviation, and from Figure 8, it can be seen that the value of the standard deviation of the IPOA is the lowest in a number of test functions, which verifies the superiority of the IPOA compared with other optimization algorithms.

In order to verify the superiority of the IPOA in a more convincing way, the Wilcoxon rank sum test is adopted to verify the difference in the algorithms using the results of the test at a certain significance level (p-value). When the p-value is less than 0.05, it indicates that there is a significant difference between the two algorithms in terms of optimization seeking performance; when the p-value is greater than 0.05, it indicates that the two algorithms

have comparable optimization seeking performance. The Table 1 shows that in CEC2017, eight benchmark test functions are selected as comparison functions, the dimension is set to 30, and each algorithm is run independently 30 times. The Wilcoxon rank sum test results of the IPOA are compared with those of GJO, SABO, POA, NGO, and SCSO.

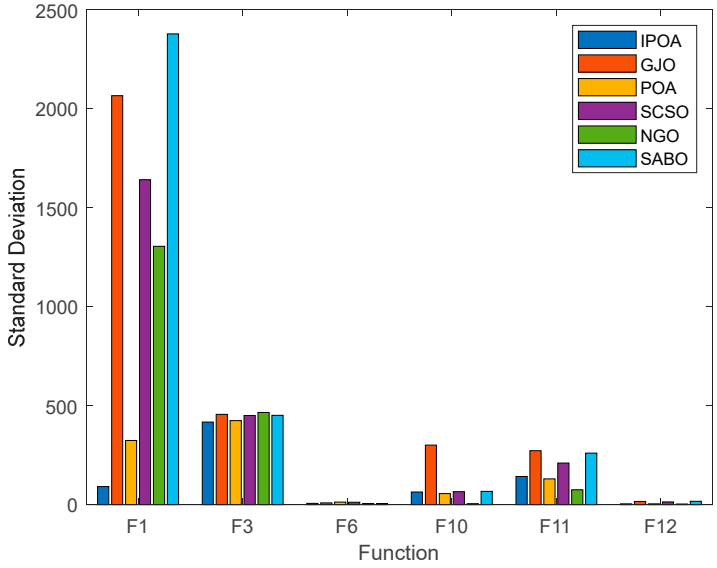


Figure 8. Standard deviation of each function solved by different algorithms.

Table 1. Wilcoxon rank sum test.

Function	*p*-Value				
	GJO	**POA**	**SCSO**	**NGO**	**SABO**
F1	3.02×10^{-11}	3.02×10^{-11}	3.02×10^{-11}	3.02×10^{-11}	3.02×10^{-11}
F3	0.070127	1.86×10^{-6}	0.510598	3.34×10^{-11}	0.000141
F4	3.34×10^{-11}	3.02×10^{-11}	3.02×10^{-11}	3.02×10^{-11}	3.02×10^{-11}
F10	4.8×10^{-7}	0.673495	6.53×10^{-8}	3.65×10^{-8}	3.02×10^{-11}
F11	3.02×10^{-11}	6.06×10^{-11}	3.69×10^{-11}	3.02×10^{-11}	3.02×10^{-11}
F12	3.02×10^{-11}	3.02×10^{-11}	3.69×10^{-11}	3.02×10^{-11}	3.02×10^{-11}
F13	6.7×10^{-11}	2.01×10^{-8}	7.6×10^{-7}	3.02×10^{-11}	3.69×10^{-11}
F14	2.96×10^{-5}	1.06×10^{-7}	0.000201	0.000587	5.57×10^{-1}

Box plots are used to reflect the center position and scattering range of a group or multiple groups of continuous-type quantitative data distributions containing mathematical statistics, which can not only analyze the level differences in different categories of data at various levels but also reveal the degree of dispersion, outliers, and distribution differences among data. The upper and lower limits of the box, respectively, are the upper and lower quartiles of the data, and the width of the box reflects the degree of fluctuation of the data to a certain extent. Several box plots are shown in Figure 9.

The change in fitness value with an increasing number of iterations is first analyzed. From the rate of change of the fitness values for solving several different functions in CEC2022, it can be seen that the IPOA has a considerable advantage over all other algorithms. Secondly, comparing the box plots of the 12 different functions in CEC2022, it is easy to see that in each function, the performance of the IPOA is optimal, and therefore, compared to other optimization-seeking algorithms, the IPOA has better convergence characteristics and higher search accuracy.

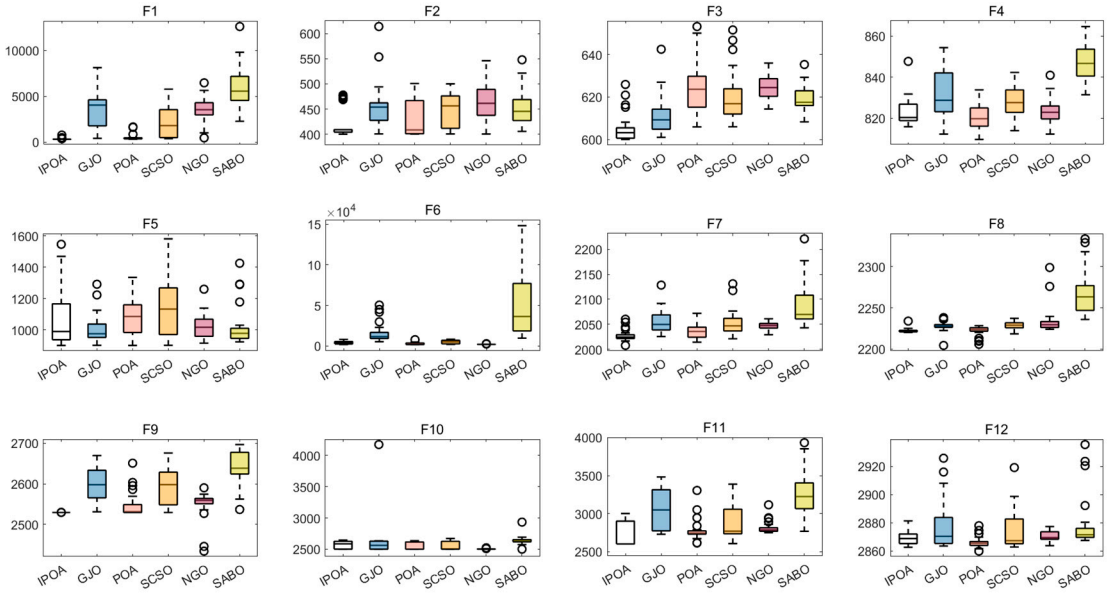


Figure 9. Box plots.

While the intuitive benefits of incorporating pumped storage for balancing wind and solar fluctuations are well understood, the uniqueness of this study lies in demonstrating how the IPOA achieves these benefits more effectively than simpler optimization models. The IPOA integrates multiple strategies—nonlinear weighting, Cauchy variation, and sparrow alert mechanisms—that allow it to dynamically adapt to the nonlinear and constrained nature of multi-energy systems.

Moreover, simpler models often focus solely on cost reduction, overlooking other critical objectives such as system stability and environmental impacts. For instance, in our case studies, the IPOA not only achieved lower costs but also significantly reduced wind and solar fluctuation rates, with reductions of up to 91.2% in curtailment rates compared to PSO. These results underscore IPOA's ability to address multi-objective trade-offs in a way that simpler models cannot.

6. Result

The calculation is based on a power grid in a certain region, which includes wind power plants, photovoltaic power plants, two hydropower stations, and three thermal power units. This article explores the impact of adding 200 MW pumped storage on various costs of the power grid and on the fluctuation rate of wind and solar power. The predicted load and new energy generation power curves for four typical days, namely in spring, summer, autumn, and winter, are shown in Figure 10.

The improved pelican optimization algorithm is used to optimize and solve the example system, where the initial population is set to 1500, the spatial dimension is 24, and the maximum number of iterations is 1000.

In order to facilitate comparative analysis of the impact of pumped storage on system costs, this article has set up eight different scenarios: Scenario 1 and Scenario 2 are typical days in spring without the pumped storage station and with the pumped storage station added, as shown in Figure 11a,b; Scenarios 3 and 4 are typical summer days without the pumped storage station and with the pumped storage station added, as shown in Figure 12a,b; Scenarios 5 and 6 are typical autumn days without the pumped storage station and with the pumped storage station added, as shown in Figure 13a,b; and Scenarios 7 and 8, respectively, show typical winter days without the pumped storage station and with the pumped storage station added, as shown in Figure 14a,b.

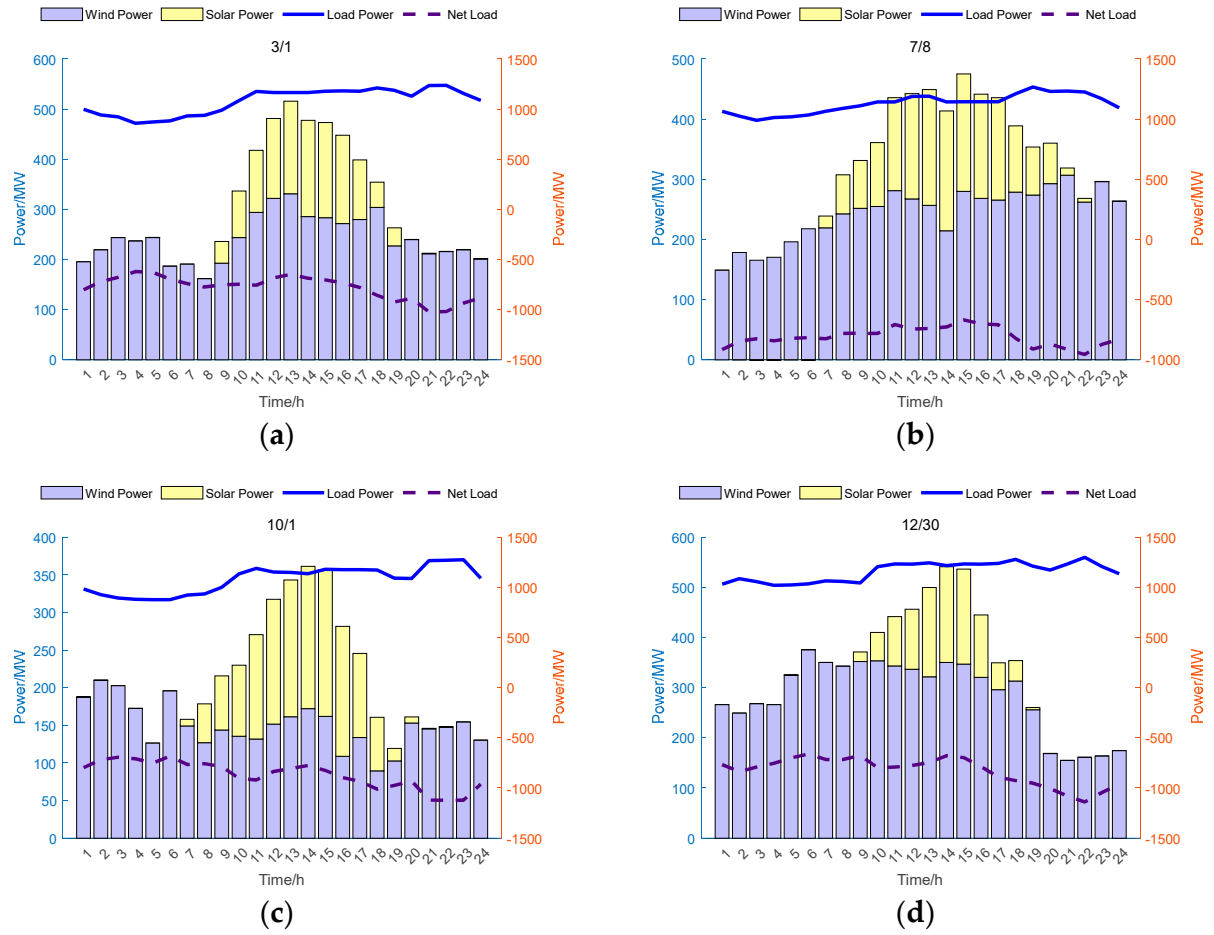


Figure 10. The predicted load and new energy generation power curves for four typical days: (**a**) spring, (**b**) summer, (**c**) autumn, (**d**) winter.

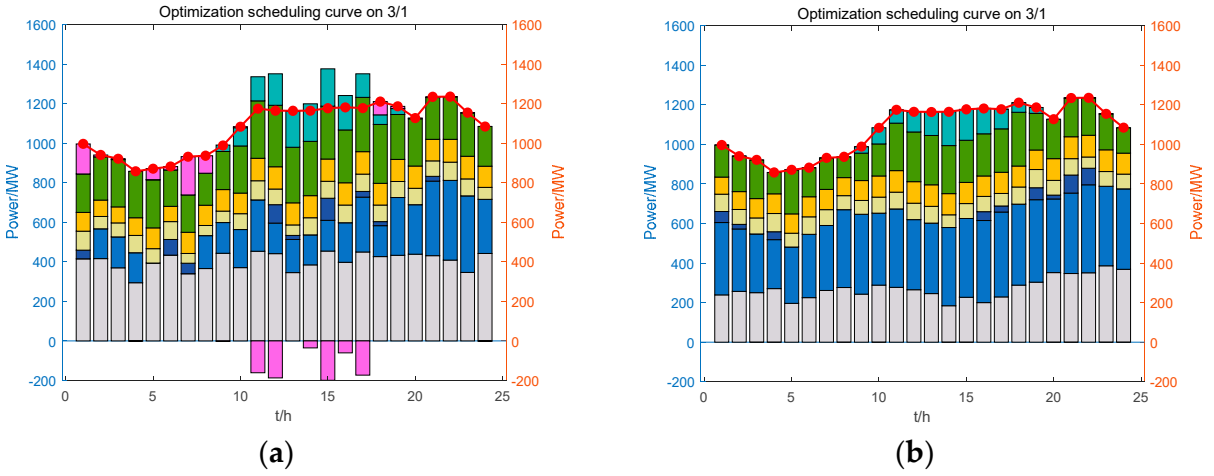
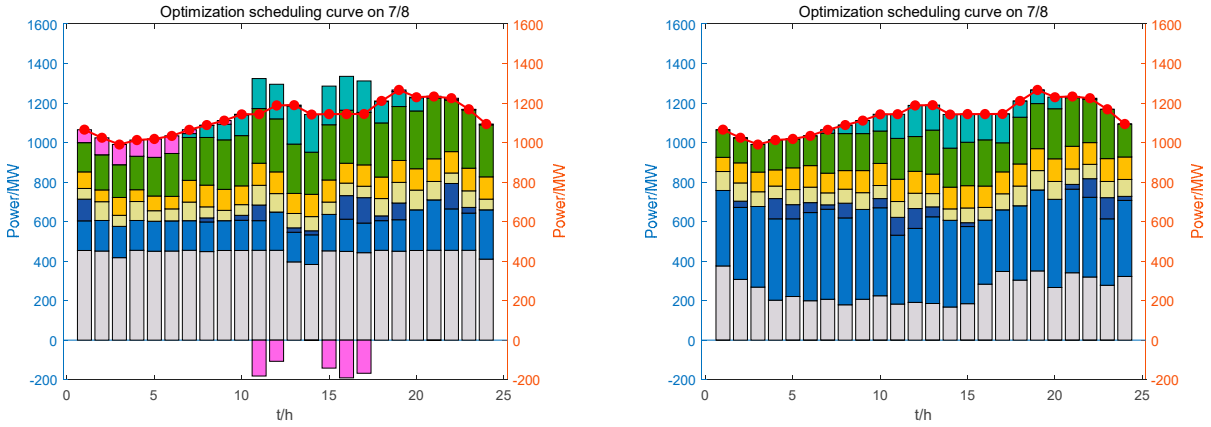


Figure 11. Optimization scheduling results for the typical day in spring: (**a**) with pumped storage power stations added; (**b**) without pumped storage power stations added.

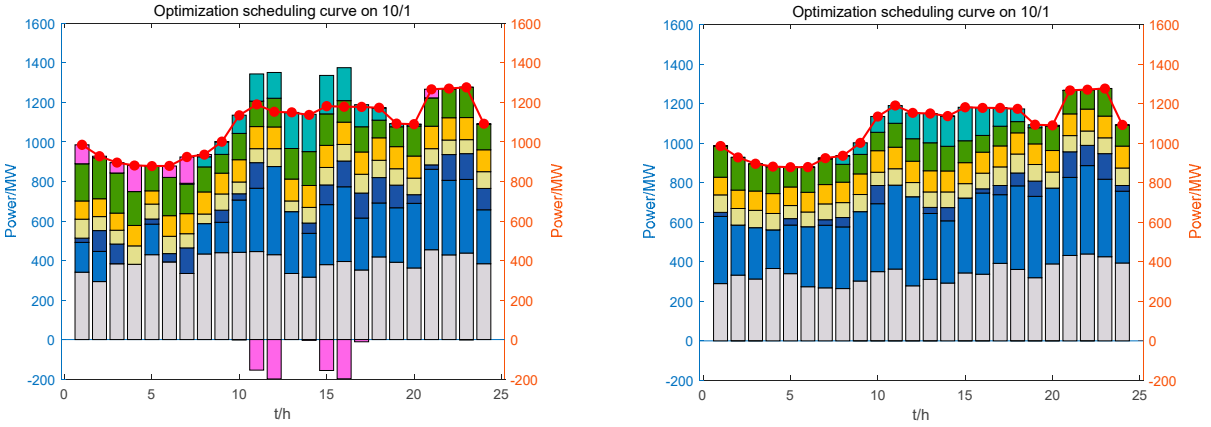
The units represented by all colors in Figures 11–14 are shown in Figure 15.

The comparison of the optimal wind and solar curtailment rate, optimal wind and solar curtailment cost, and optimal cost obtained through optimization using different algorithms for four typical days is shown in Table 2.



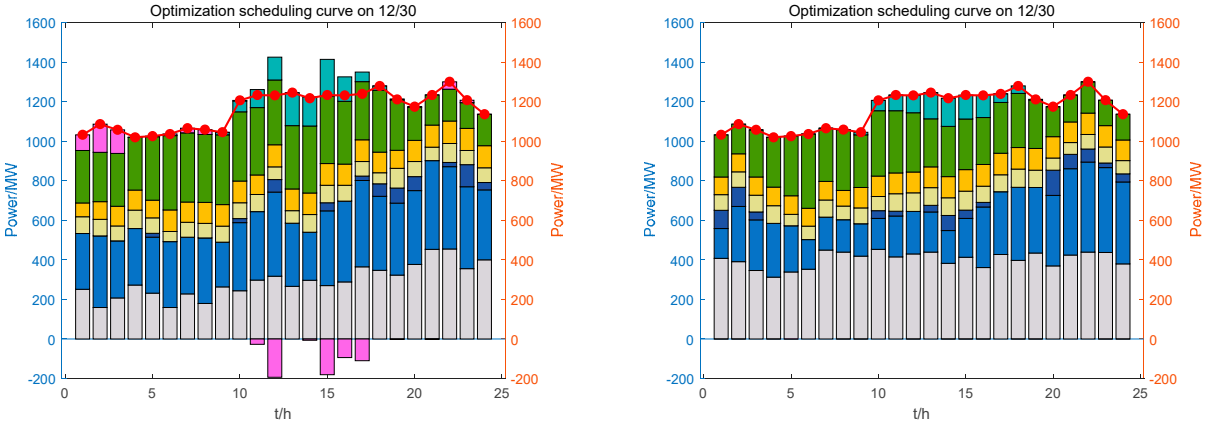
(**a**) (**b**)

Figure 12. Optimization scheduling results for the typical day in summer: (**a**) with pumped storage power stations added; (**b**) without pumped storage power stations added.



(**a**) (**b**)

Figure 13. Optimization scheduling results for the typical day in autumn: (**a**) with pumped storage power stations added; (**b**) without pumped storage power stations added.



(**a**) (**b**)

Figure 14. Optimization scheduling results for the typical day in winter: (**a**) with pumped storage power stations added; (**b**) without pumped storage power stations added.

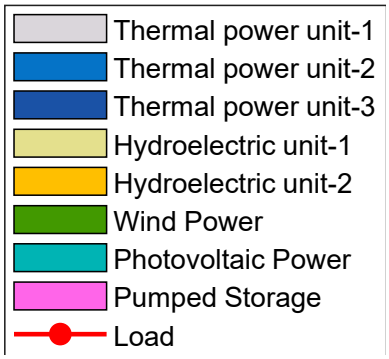


Figure 15. The units represented by each color in Figures 11–14.

Table 2. Comparison of the results of optimal curtailment of wind and solar power and cost under different algorithms.

Typical Days	Algorithms	Optimal Curtailment Rate of Solar and Wind (%)		Optimal Curtailment Cost of Solar and Wind (CNY 10,000)		Optimal Cost (CNY 10,000)	
Has the Pumped Storage Station Been Added?		Yes	No	Yes	No	Yes	No
March 1st	PSO	5.41	21.91	46.44	188.51	4765.76	5009.53
	WGO	1.42	16.68	12.09	143.48	4712.53	4986.83
	POA	5.51	23.91	47.52	205.72	4939.95	5140.44
	IPOA	0.48	16.27	4.16	139.98	4674.12	4943.96
July 8th	PSO	4.3	24.1	39.47	221.41	4564.25	4852.55
	WGO	2.72	21.33	24.99	195.94	4549.17	4842.22
	POA	5.5	24.63	50.46	226.28	4699.35	5017.98
	IPOA	0.88	19.38	8.07	178.01	4476.84	4753.52
October 1st	PSO	6.13	26.01	37.32	158.4	3386.21	3564.31
	WGO	4.64	27.89	28.23	169.85	3303.01	3589.93
	POA	7.72	23.44	46.98	142.75	3442.66	3649.74
	IPOA	1.64	22.15	9.97	134.87	3275.62	3433.02
December 30th	PSO	3.45	19.7	32.87	187.62	5135.07	5418.25
	WGO	1.14	18.84	10.83	179.45	5092.47	5387.36
	POA	3.35	21.26	31.91	202.55	5344.79	5511.93
	IPOA	0.52	16.64	4.96	148.46	5060.81	5233.03

By comparing the various data from the POA and IPOA, it can be seen that with the addition of pumped storage, on the typical day in spring, the curtailment rate and cost of wind and solar energy decreased by 91.2%, and the cost decreased by CNY 2.6583 million. On the typical day in summer, the curtailment rate and cost of wind and solar decreased by 84% and CNY 2.2251 million, respectively. On the typical day in autumn, the curtailment rate and cost of wind and light decreased by 78.75% and CNY 1.6704 million, respectively. On the typical day in winter, the curtailment rate of wind and solar energy decreased by 84.47%, respectively, with a cost reduction of CNY 2.8398 million. Compared with various algorithms, the results of the curtailment of wind and solar energy optimized by the IPOA are the best, as well as the cost of the system.

Four compromise solutions were selected from the Pareto front, which are the objective functions (the cost and the standard deviation of wind and solar fluctuations) for four typical days optimized by the IPOA, as shown in the Table 3.

Under the selected four typical day scenarios, the optimization objectives were analyzed. The results showed that on the typical day in spring, with and without pumped storage, the cost was reduced by CNY 1.0296 million, and the standard deviation of wind and solar fluctuations was reduced by 23.8%. During the typical day in summer, the cost

decreased by CNY 6.853 million with and without pumped storage, and the standard deviation of wind and solar fluctuations decreased by 29.31%. In the typical day of autumn, with or without pumped storage, the cost decreased by CNY 4.895 million, and the standard deviation of wind and solar fluctuations decreased by 7.738%. On the typical day in winter, with or without pumped storage, the cost decreased by CNY 5.886 million, and the standard deviation of wind and solar fluctuations decreased by 13.11%.

Table 3. Objective function analysis of four typical daily scenarios optimized by the IPOA.

Typical Days	Cost (CNY 10,000)		Standard Deviation of Wind and Solar Fluctuations (MW)	
	Pumped Storage Station Added	Without Pumped Storage Station	Pumped Storage Station Added	Without Pumped Storage Station
March 1st	4841	4943.96	70.5768	92.622
July 8th	4678.9	5364.2	56.6084	80.085
October 1st	3408.5	3898	58.3075	63.1983
December 30th	5243.7	5832.3	80.4436	92.5799

7. Discussion

This study highlights the methodological advancements achieved through the improved pelican optimization algorithm (IPOA) for optimizing multi-energy complementary systems. By integrating nonlinear weighting, Cauchy variation, and the sparrow alert mechanism, the IPOA provides a robust framework for addressing the dynamic, nonlinear, and multi-constraint nature of renewable energy systems. Methodologically, these enhancements not only improve solution accuracy and convergence speed but also contribute to the development of more adaptive optimization techniques that can be applied across various domains, such as smart grid management and real-time energy dispatch.

From a policy perspective, the findings offer actionable insights for energy planners and policymakers. The demonstrated ability of the IPOA to minimize operational costs, reduce wind and solar curtailment, and enhance system stability underscores its potential to facilitate the large-scale integration of renewable energy. Policymakers can leverage these results to promote investments in pumped storage systems and advanced optimization technologies, ensuring more sustainable and resilient energy infrastructures. Furthermore, the study highlights the importance of balancing economic efficiency with environmental goals, providing a quantitative basis for developing policies that align with carbon neutrality objectives.

In this study, the IPOA demonstrated significant advantages over other algorithms, such as PSO, WGO, and POA. For example, on the typical spring day, the IPOA reduced wind and solar curtailment rates by 91.2% compared to PSO and 66.2% compared to WGO, while achieving a cost reduction of CNY 2.6583 million compared to traditional methods. Across all scenarios, the IPOA consistently showed lower standard deviations in wind and solar fluctuations, indicating improved stability.

These results highlight the IPOA's potential for optimizing renewable energy systems, particularly in scenarios with complex constraints and multi-objective demands. In practice, IPOA's superior performance could contribute to the efficient integration of large-scale renewable energy into power grids, reducing operational costs and enhancing system reliability.

Future work will focus on extending the IPOA to dynamic, real-time energy dispatch scenarios. Additionally, integrating the IPOA with advanced technologies like artificial intelligence (AI) and the Internet of Things (IoT) could further enhance the adaptability

and intelligence of power system management. This includes applications in predictive analytics and self-learning energy dispatch systems, paving the way for smarter, more sustainable grid solutions.

Author Contributions: Conceptualization, H.Z. and F.W.; data curation, J.C.; formal analysis, J.C.; funding acquisition, C.Y.; investigation, Y.L.; methodology, J.C.; project administration, H.Z.; resources, J.C.; software, J.C.; supervision, J.Y.; validation, H.Z., J.C. and F.W.; visualization, H.Z.; writing—original draft, J.C.; writing—review and editing, J.C. and F.W. All authors have read and agreed to the published version of the manuscript.

Funding: This research received no external funding.

Data Availability Statement: The raw data supporting the conclusions of this article will be made available by the authors on request.

Acknowledgments: The authors would like to acknowledge Fushuan Wen for his invaluable support and guidance throughout this research and Hongbo Zou for his assistance as well. Acknowledgment is given to the Hainan Institute of Zhejiang University for their assistance with this research, and to Haotong Han from Liaoning Technical University for his valuable suggestions regarding the research work.

Conflicts of Interest: The funders had no role in the design of the study; in the collection, analyses, interpretation of data; in the writing of the manuscript; or in the decision to publish the results.

References

1. Cui, D.; Xu, F.; Ge, W.; Huang, P.; Zhou, Y. A coordinated dispatching model considering generation and operation reserve in wind power-photovoltaic-pumped storage system. *Energies* **2020**, *13*, 4834. [CrossRef]
2. Chen, C.; Liu, H.; Xiao, Y.; Zhu, F.; Ding, L.; Yang, F. Power generation scheduling for a hydro-wind-solar hybrid system: A systematic survey and prospect. *Energies* **2022**, *15*, 8747. [CrossRef]
3. Zhang, J.; Ji, X.; Ren, Y.; Yang, J.; Qiao, Y.; Jin, X.; Yao, S.; Qiao, R. IASA-based capacity allocation optimization study for a hydro–pumped storage–photovoltaic–wind complementary clean energy base. *Front. Energy Res.* **2022**, *10*, 891225. [CrossRef]
4. Zhao, L.; Zeng, Y.; Peng, D.; Li, Y. Optimal Economic Allocation Strategy for Hybrid Energy Storage System under the Requirement of Wind Power Fluctuation. In Proceedings of the 2023 IEEE Power & Energy Society General Meeting (PESGM), Orlando, FL, USA, 16–20 July 2023. [CrossRef]
5. Zhang, Z.; Wang, Z.; Cao, R.; Zhang, H. Research on two-level energy optimized dispatching strategy of microgrid cluster based on IPSO algorithm. *IEEE Access* **2021**, *9*, 120492–120501. [CrossRef]
6. Zhu, Y.; Yao, S.; Zhang, Y.; Cao, M. Environmental and economic scheduling for wind-pumped storage-thermal integrated energy system based on priority ranking. *Electr. Power Syst. Res.* **2024**, *231*, 110353. [CrossRef]
7. Yang, X.; Long, J.; Liu, P.; Zhang, X.; Liu, X. Optimal scheduling of microgrid with distributed power based on water cycle algorithm. *Energies* **2018**, *11*, 2381. [CrossRef]
8. Dai, J.; Dong, H. Research on the capacity optimization of the wind-solar hybrid power supply system based on pumped storage power station. *Power Syst. Clean Energy* **2019**, *35*, 76–82.
9. Abdolrasol, M.G.; Mohamed, R.; Hannan, M.A.; Al-Shetwi, A.Q.; Mansor, M.; Blaabjerg, F. Artificial neural network based particle swarm optimization for microgrid optimal energy scheduling. *IEEE Trans. Power Electron.* **2021**, *36*, 12151–12157. [CrossRef]
10. Wang, Y.; Liu, J. Optimal capacity allocation of wind-light-water multi-energy complementary capacity based on improved multi-objective optimization algorithm. *Front. Energy Res.* **2023**, *10*, 1115769. [CrossRef]
11. Wang, K.; Ge, P.; Duan, N.; Wang, J.; Lv, J.; Liu, M.; Wang, B. The Multi-Objective Optimal Scheduling of the Water–Wind–Light Complementary System Based on an Improved Pigeon Flock Algorithm. *Energies* **2023**, *16*, 6787. [CrossRef]
12. Shi, M.; Wang, W.; Han, Y.; Huang, Y. Research on comprehensive benefit of hydrogen storage in microgrid system. *Renew. Energy* **2022**, *194*, 621–635. [CrossRef]
13. Liang, Z.; Chung, C.Y.; Zhang, W.; Wang, Q.; Lin, W.; Wang, C. Enabling High-Efficiency Economic Dispatch of Hybrid AC/DC Networked Microgrids: Steady-State Convex Bi-Directional Converter Models. *IEEE Trans. Smart Grid* **2025**, *16*, 45–61. [CrossRef]
14. Yi, L.; Li, G.; Chen, K.; Liu, J.; Fan, L.; Gao, X. Optimal scheduling of intelligent building with photovoltaic energy storage system using competitive mechanism integrated multi-objective equilibrium optimizer algorithm. *Arab. J. Sci. Eng.* **2022**, *47*, 14641–14655. [CrossRef]

15. Qiu, Y.; Zhao, J.; Nian, H.; Xu, J. Research on Multi-objective Optimal Scheduling Strategy of Renewable Energy Distribution Networks. In Proceedings of the 2022 4th International Conference on Electrical Engineering and Control Technologies (CEECT), Shanghai, China, 16–18 December 2022; pp. 816–821. [CrossRef]
16. Ghanbari, K.; Maleki, A.; Ochbelagh, D.R. Optimal design of solar/wind/energy storage system-powered RO desalination unit: Single and multi-objective optimization. *Energy Convers. Manag.* **2024**, *315*, 118768. [CrossRef]
17. Ma, H.; Tian, H.; Zhang, K.; Liu, Y. An Optimal Scheduling Strategy for Wind-PV and Multi-Type Energy Storage Co-Generation System. In Proceedings of the 2023 6th International Conference on Power and Energy Applications (ICPEA), Weihai, China, 24–26 November 2023. [CrossRef]
18. Bao, Z.; Zhou, Q.; Yang, Z.; Yang, Q.; Xu, L.; Wu, T. A multi time-scale and multi energy-type coordinated microgrid scheduling solution—Part I: Model and methodology. *IEEE Trans. Power Syst.* **2014**, *30*, 2257–2266. [CrossRef]
19. He, Y.-L.; Wu, X.-W.; Sun, K.; Liu, X.-Y.; Wang, H.-P.; Zeng, S.-M.; Zhang, Y. A Novel MOWSO algorithm for Microgrid multi-objective optimal dispatch. *Electr. Power Syst. Res.* **2024**, *232*, 110374. [CrossRef]
20. Li, Y.; Yang, Z.; Li, G.; Zhao, D.; Tian, W. Optimal scheduling of an isolated microgrid with battery storage considering load and renewable generation uncertainties. *IEEE Trans. Ind. Electron.* **2018**, *66*, 1565–1575. [CrossRef]
21. Wang, Z.; Fang, G.; Wen, X.; Tan, Q.; Zhang, P.; Liu, Z. Coordinated operation of conventional hydropower plants as hybrid pumped storage hydropower with wind and photovoltaic plants. *Energy Convers. Manag.* **2023**, *277*, 116654. [CrossRef]
22. Luo, S.; Peng, K.; Hu, C.; Ma, R. Consensus-Based Distributed Optimal Dispatch of Integrated Energy Microgrid. *Electronics* **2023**, *12*, 1468. [CrossRef]
23. Bo, Y.; Xia, Y.; Wei, W.; Li, Z.; Zhao, B.; Lv, Z. Hyperfine optimal dispatch for integrated energy microgrid considering uncertainty. *Appl. Energy* **2023**, *334*, 120637. [CrossRef]
24. Nwulu, N.I.; Xia, X. Optimal dispatch for a microgrid incorporating renewables and demand response. *Renew. Energy* **2017**, *101*, 16–28. [CrossRef]
25. Tian, L.; Cheng, L.; Guo, J.; Wu, K. System modeling and optimal dispatching of multi-energy microgrid with energy storage. *J. Mod. Power Syst. Clean Energy* **2020**, *8*, 809–819. [CrossRef]

Disclaimer/Publisher's Note: The statements, opinions and data contained in all publications are solely those of the individual author(s) and contributor(s) and not of MDPI and/or the editor(s). MDPI and/or the editor(s) disclaim responsibility for any injury to people or property resulting from any ideas, methods, instructions or products referred to in the content.